JIPB Journal of Integrative Plant Biology

Research Article
https://doi.org/10.1111/jipb.13753

Proteomic dynamics revealed sex-biased responses to combined heat-drought stress in *Marchantia*[∞∞]

Sara Guerrero, Víctor Roces, Lara García-Campa, Luis Valledor and Mónica Meijón*

Department of Organisms and, Systems Biology, Faculty of Biology/Biotechnology, Institute of Asturias, University of Oviedo, Oviedo, Asturias 33071, Spain

*Correspondence: Mónica Meijón (meijonmonica@uniovi.es)

Sara Guerrero

Mónica Meijón

ABSTRACT

Recent studies have documented plant responses to climate change extensively, particularly to single-stress exposures. However, critical factors for stress survival, such as sexual differentiation, are not often considered. The dioicous *Marchantia polymorpha* stands as an evolutionary milestone, potentially preserving ancestral traits from the early colonizers. In this study, we employed proteomic analyses complemented with physiological monitoring to investigate combined heat and drought responses in Tak-1 (male) and Tak-2 (female) accessions of this liverwort. Additionally, targeted transcriptomics was conducted using different natural populations from contrasting environments. Our findings revealed sex-biased dynamics among natural accessions, particularly evident under control conditions and during early stress responses. Although Tak-2 exhibited greater diversity than Tak-1 under control conditions, male accession demonstrated distinct and more rapid stress sensing and signaling. These differences in stress response appeared to be strongly related to sex-specific plasticity influenced by geoclimatic origin. Furthermore, we established distinct protein gene ages and genomic distribution trends, underscoring the importance of protein diversification over time. This study provides an evolutionary perspective on sexual divergence and stress emergence employing a systems biology approach, which allowed for the establishment of global and sex-specific interaction networks in the stress response.

Keywords: abiotic stress, land adaptation, liverwort, sex-biased response, systems biology

Guerrero, S., Roces, V., García-Campa, L., Valledor, L., and Meijón, M. (2024). Proteomic dynamics revealed sex-biased responses to combined heat-drought stress in *Marchantia*. J. Integr. Plant Biol. **66:** 2226–2241.

INTRODUCTION

Environmental fluctuations exert selective pressure on plants as sessile organisms, potentially resulting in irreversible and irreparable consequences when occurring rapidly, intensely and unexpectedly. Climate change has already caused shifts in the local distribution of some species that are unable to cope with such perturbations and adapt. Looking ahead, this scenario is expected to drive the evolutionary trajectory of plant species, not only by reshaping their diversity but also by favoring the selection of genotypes with resistant traits (Parmesan and Yohe, 2003; Thuiller et al., 2005).

Remarkable advancements in understanding plant sensing and response have emerged in recent years, which are pivotal for preventing damage, maintaining homeostasis and ensuring survival. Signaling and protective mechanisms overlap across various climate change stresses (heat, drought, UV) and have been documented extensively. Phytohormone-like compounds, soluble sugars and reactive oxygen species (ROS) act as stress sensors, while the response to stress includes photosynthetic

inhibition, changes in membrane fluidity, accumulation of antioxidants and protein denaturation. Furthermore, these properties can be influenced by diverse biological factors. For example, polymorphic variations in ROS-related sensors impact water stress responses, highlighting the importance of natural variation for stress survival (Bigot et al., 2018). However, many aspects remain to be investigated regarding the interplay of these elements and stresses, and whether plants will possess the capacity to adapt to the new environmental conditions already underway.

The model liverwort *Marchantia polymorpha* represents an evolutionary milestone, potentially retaining ancestral traits from the early colonizers. It has developed essential mechanisms to withstand extreme terrestrial fluctuations with low plant complexity (Clark et al., 2023), making it a valuable tool for deciphering response mechanisms to hostile conditions and providing a crucial evolutionary perspective. Among its innovations, discoveries include cell wall integrity for controlling water balance, light and temperature protection through diverse photoreceptors and phytohormone regulation, all of which are revealed as crucial evolutionary steps (Bowman et al., 2017).

Previous studies in *M. polymorpha* have revealed targeted responses to abiotic stress, highlighting both epigenetic (DNA, histones, chromatin remodeling, and microRNAs) and genetic (heat shock factors and late embryogenesis abundant proteins) factors. Additionally, specific hormone roles including oxylipins and abscisic acid have been involved in efficient stress responses (Akter et al., 2014; Marchetti et al., 2021). However, holistic understanding, predicting and overcoming stress effects will only come from systems biology research. Recently, extensive datasets of stress responses in this species have been produced (Carella et al., 2019; Wu et al., 2022a, 2022b; Tan et al., 2023). Nevertheless, there is scarce information covering combined heat and drought stress responses, which appeared to have distinctive effects from a single drought or heat in other plants, not following simple additive trends (Rizhsky et al., 2004). Proteomics has been widely used to study abiotic stress, considering the direct effect of the proteome as the driver of whole plant response, linking physiology, metabolic changes, gene regulation and translation machinery (Kosová et al., 2011).

This species features one of the most ancient sexual differentiation systems, with U as the female and V as the male sex chromosomes. Both sexual genotypes have adapted to surface conditions, representing a pivotal point in the perpetuation and development of modern species (Bowman et al., 2017; Wu et al., 2022a). Transcriptomic analyses across various algae species have associated differences in female and male morphology and physiology with sex-biased gene expression, likely stemming from distinct reproductive costs (Hatchett et al., 2023). Despite the direct impact of sex on plant survival and evolution itself, the potential divergent effects of climate change on crucial factors like sex have not been frequently explored. Consistent studies have demonstrated a substantial influence of sexual differentiation on stress responses in diverse plant species, potentially linked to sex-specific traits and purposes (Juvany and Munné-Bosch, 2015).

Hence, our investigation aimed to uncover how *Marchantia* accessions responded to simultaneous heat and drought stress. Specifically, we sought to determine whether sex played a role in the ability of plants to endure future climate conditions. If so, we aimed to explore the mechanisms underlying those differences and assess whether natural variation could contribute to sex-biased trends, thereby influencing overall survival. Here, we report sex-biased differences in response to combined heat and drought stress in natural accessions of *M. polymorpha* at physiological, gene and proteomic levels. Stress differentiation between sex genotypes appeared to be strongly influenced by the geographic origin of the population. Sex-specific plasticity could play a crucial role in stress survival when a strong restructuring response is needed.

RESULTS

Overall physiological responses to combined heat-drought stress indicated a potential stronger shock on Tak-2 compared to Tak-1

A time-course experiment of combined heat and drought stress was conducted on thalli from Tak-1 (male) and Tak-2 (female) accessions from *M. polymorpha*. Different treatment intervals were considered: before the first stress shock (control, C) and after first (T1, first day), second (T2, second day) and third (T3, third day) daily combined stress intervals. These intervals consisted of heat shocks at 27°C for 2 h, coupled with progressive drought resulting in approximately a 15% reduction in soil water content (SWC) during each daily stress pulse (see Materials and Methods).

Gradual phenotypic changes were observed in both accessions, Tak-1 (male) and Tak-2 (female), during the time-course stress exposure, such as visible dehydration (Figure 1A). A decrease in photosynthetic activity, supported by F_v/F_m measurements, was also monitored throughout the experiment (Figure 1A; Table S1). Low photosynthetic values at the T3 stress time resulted in non-survival of individuals during post-stress recovery. Nevertheless, viable gemmae were produced, which grew after the stress (Figure S1). Although the overall response trends between accessions were similar, a potentially earlier or stronger stress response of Tak-1 could be inferred from phenotypic and photosynthetic damages after shorter-term T1 stress exposure.

Photosynthetic pigment quantification at control and T1 and T2 stress times (T3 was not considered due to very low photosynthetic activity, which was probably related to senescence) reinforced stress differences between accessions (Figure 1B; Table S1). Tak-1 showed a decrease in chlorophyll *a* and *b* content and an increase in carotenoids as a T1 response, contrary to Tak-2, which did not exhibit that early response. Moreover, although both accessions showed similar tendencies in some stress markers such as

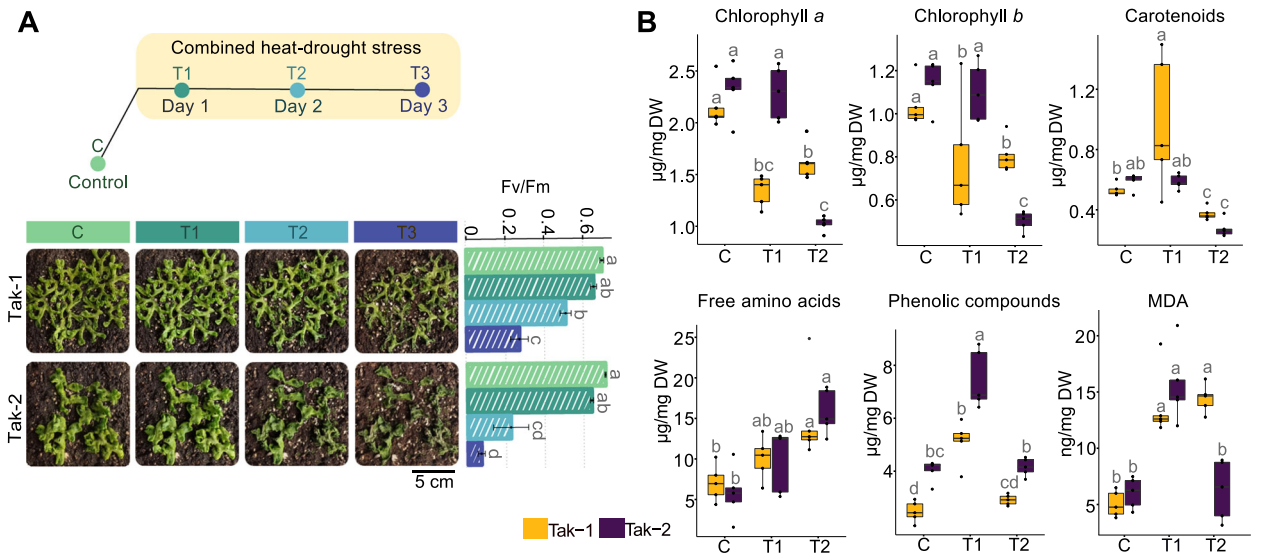

Figure 1. Phenotypic and physiological monitoring by a combined heat and drought experiment in *Marchantia polymorpha* thalli (Tak-1 and Tak-2)

(A) Phenotypical changes during stress as well as maximal efficiency of photosystem II (F_v/F_m) measurements at stress times (mean ± SD). **(B)** Biochemical marker quantification (C, T1, and T2), from left to right, chlorophylls *a* and *b*, carotenoids, free amino acids, total phenolic compounds and malondialdehyde (MDA). Different letters indicate significant differences between treatments or accessions ($P < 0.05$). C as control and T1, T2, and T3 as first, second and third daily combined stress intervals, respectively.

the accumulation of free amino acids and total phenolic compounds (Figure 1B; Table S1), MDA differed between accessions, with Tak-2 individuals exhibiting decreased levels at longer term T2.

Distinct protein dynamics between accessions were revealed, highlighting processes behind the quicker response of Tak-1

Complex phenotypic and physiological responses to environmental stresses result from elaborated molecular restructuring processes. To gain an in-depth understanding of the accession' behaviors during combined heat and drought, proteomic analysis was conducted on Tak-1 and Tak-2 accessions at selected control, T1 and T2 treatment times. T3 was associated with senescence processes due to very low photosynthetic activity and was therefore not considered. Out of the total proteins identified using nLC-Orbitrap/MS, 3577 proteins met pre-established criteria for analyses (Table S2, see Materials and Methods).

Specific proteomic profiles for each accession on the time-course stress experiment were established. Comparing Tak-1 (Figure 2A) and Tak-2 (Figure 2B), Tak-2 presented more exclusive proteins belonging to a more diverse range of functional categories under control conditions. However, it reduced the number of qualitative proteins by two or three times when stress was involved. In contrast, Tak-1 showed a greater collection of proteins during stressful times similar to or surpassing their control state but with a redistribution across functional categories.

Protein dynamics, as established by heatmap representation, showed a mismatch in the stress responses of Tak-1 (Figure 2C) and Tak-2 (Figure 2D). Both accessions began to decrease proteins associated with active growth and development (e.g., multi-process regulation, cell division) as a response to T1 stress. Both accessions seemed to be regulating redox homeostasis at T2 stress time. However, only Tak-1 exhibited an increase in proteins related to RNA and protein remodeling machineries, specific metabolisms (nucleotide, amino acid, lipid, and carbohydrate) and cellular respiration as a short-term T1 response. Tak-2 showed a similar response, but it occurred at the longer term T2 stress time. Heatmap hierarchical clustering and differential analysis supported these results (Table S2), with Tak-1 clustering together stress periods with more differential proteins between control and stress times (Figure 2C), in contrast with Tak-2, which clustered together control and T1 stress periods with more differential proteins between T1 and T2 stress times (Figure 2D).

To delve into specific protein trends, 15 protein clusters were classified using a K-means approach (Figure 2E; Table S2). While some clusters were linked to shared patterns in both accessions, such as clusters 6, 10, 11, and 14, most of them were accession-dependent, revealing differences between accessions at control or under stress. Both accessions showed protein degradation during stress, as evidenced by free amino acid accumulation (Figure 1B), enrichment of cluster 7 with proteolytic aspartic-type peptidase activities and enrichment of cluster 11 with amino acid lysine degradation. However, protein biosynthesis and modification appeared to differentiate between the two accessions, particularly at the shorter-term T1. Clusters 5 and 12 showed that Tak-1 increased proteins related to the biosynthesis of aspartate-derived amino acids, ribosomal subunits and plastid components as well as proteins related to modification by cyclophilins

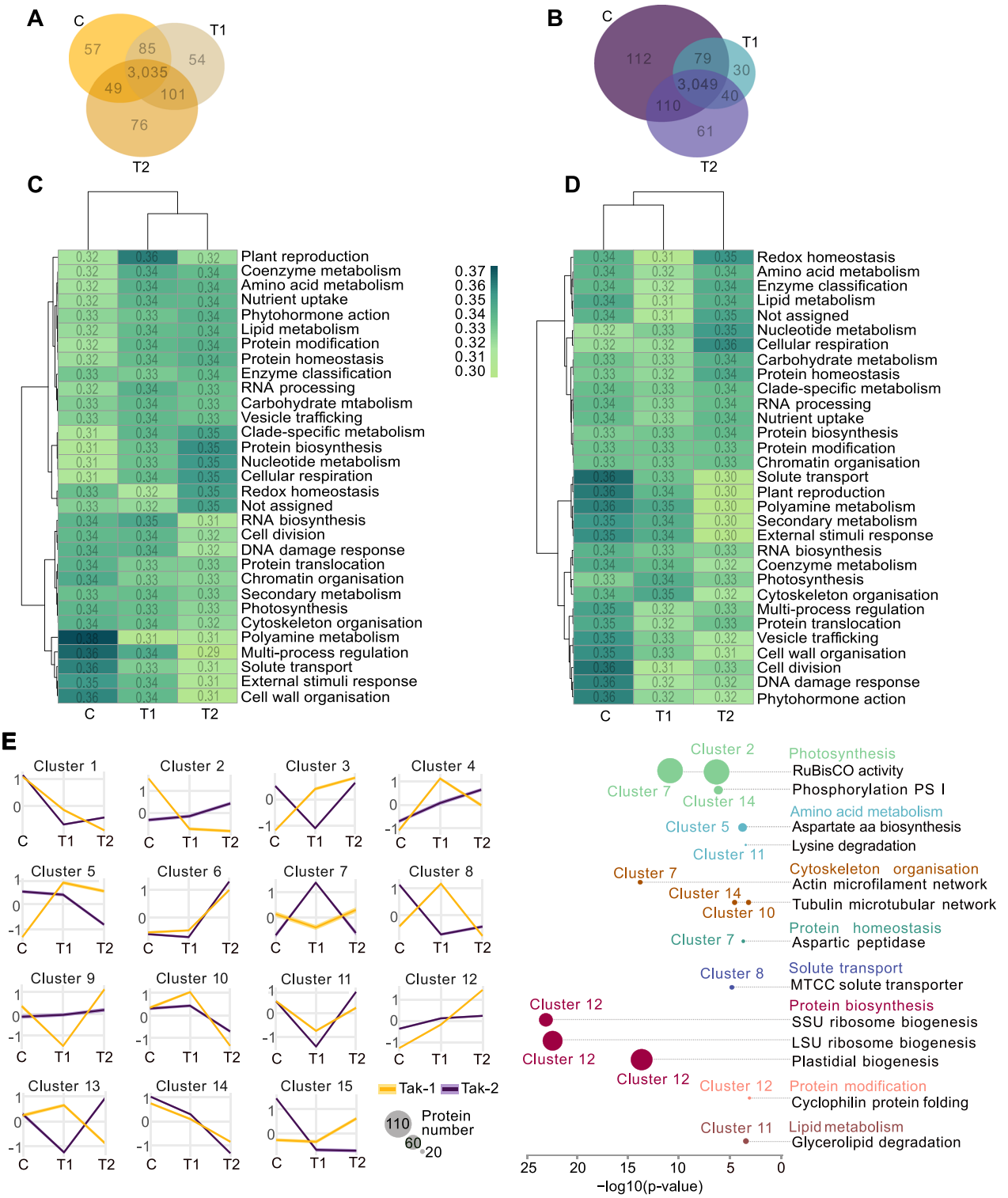

Figure 2. Functional dynamics in proteomic data throughout the experiment

(A) and **(B)** Venn diagrams for Tak-1 in yellow and Tak-2 in purple, respectively, each treatment circle scaled by the number of proteins represented. **(C)** and **(D)** Heatmap/hierarchical clustering using Mercator4 categorization pathways for Tak-1 and Tak-2, respectively, with numbers indicating scaled abundance by rows. **(E)** *K*-means protein clustering in 15 groups (top panel, with dispersion range in lighter yellow or purple for Tak-1 or Tak-2, respectively) and MapMan functional enrichments (bottom panel) of enriched clustered groups displaying significant *P*-values ($P < 0.05$), with each enrichment dot scaled by the number of proteins represented. C as control and T1 and T2 as first and second daily combined stress intervals, respectively.

at T1. Furthermore, differences in photosynthesis were highlighted by clusters 2 and 7, where only Tak-1 decreased photosynthetic proteins enriched in ribulose-1,5-bisphosphat carboxylase/oxygenase (RuBisCO) at T1. This could support the decrease in chlorophyll *a* and *b* content observed earlier in Tak-1 (Figure 1). Lastly, solute transport enrichment in cluster 8 could indicate a difference, showing variations between control and shorter-term T1 between accessions, with Tak-1 increasing related proteins compared with the control and Tak-2 drastically decreasing them.

Stress dependent- and independent-accession identities were elucidated

Both accessions presented significant proteomic variability not only in response to stress (particularly T1) but also in their control identity (Figure 2). To discern the main sources of variation in the data, MOFA2 inference analysis was conducted using a general framework.

Latent factor 1 (LF1) captured the greatest variation distinguishing between accessions (3.32%), indicating that the main source of proteome variation is the distinction between genotypes rather than stress times (Figures 3A, S2A; Table S3). Tak-1 was enriched in cell wall organization and cellular respiration, while Tak-2 was enriched in enzyme classification and redox homeostasis. Most of the variables with the highest weights were related to Tak-2, with only a few strong variables associated with Tak-1. Latent factor 2 (LF2) tended to separate T2 response regardless of genotype (1.51%). Its differentiation presented strong biomarkers such as CHAPERONE COMPONENT CLPD OF CHLOROPLAST CLP-TYPE PROTEASE COMPLEX (ClpC), WDL microtubule stabilizing factor (WDL) and MITOCHONDRIAL IMPORT INNER MEMBRANE TRANSLOCASE (TIM23) (Figure 3B). Latent factor 3 (LF3) established a clear differentiation between all analyzed stress times only in Tak-1 (1.36%), with top variables related to solute transport (TONOPLAST INTRINSIC PROTEIN, TIP), protein biosynthesis (AMINOACYL-TRNA BINDING FACTOR, EEF1A) and cell wall (PROBABLE XYLOGLUCAN ENDOTRANSGLUCOSYLASE HYDROLASE, XET) (Figure 3B).

Essential genotype characteristics are crucial for post-stress development and for distinctive stress responses, as demonstrated. To examine how identity commitment varies throughout the stress, a multi-group framework of MOFA2 was carried out, with the analyzed times as supervised groups (control, T1, and T2).

More explained variation was found at control time (9.12%), decreasing at T1 (4.53%) and T2 (5.36%) (Figure 3C; Table S3). Latent factor 1' (LF1') explained the greatest variation (13.75%) associated with genotype separation in all time groups (Figure S2B), presenting genotypic markers potentially linked to differential responses and essential characteristics (Figure 3D). Among the Tak-1 markers, CYTOSOLIC POLYAMINE OXIDASE (PAO), LEUCINE-RICH REPEAT MDIS1-INTERACTING RECEPTOR-LIKE KINASES 2 (MIK2), PP5 PHOSPHATASE (PP5) and a SERINE/THREONINE PROTEIN PHOSPHATASE (PP1) located on the V clearly allowed its distinction. Among the Tak-2 markers, two FB LECTIN (FBL) and SNOAL-LIKE DOMAIN (NTF2) enabled its distinction (Figure 3E).

Potential protein interactions related to differential stress response between Tak-1 and Tak-2 were revealed

Previous results suggest that functional divergence among accessions may be linked to different protein interactions. To explore this further, protein meta-networks and module enrichments were conducted for each accession.

Differences in interacting proteins were identified between accessions, particularly in relation to most regulatory proteins by Katz centrality (Table S4). In Tak-1, proteins involved in gene regulation and sensing, such as *S*-ADENOSYL HOMOCYSTEINE HYDROLASE (SAHH) and MAPK KINASE (MPK3/6) were observed (Figure 4A). SAHH showed numerous interacting edges in this accession, including LYSINE N-METHYLTRANSFERASE (RuBisCO LSMT) involved in RuBisCO regulation, COMPONENT SF3A1 OF SPLICING FACTOR 3A COMPLEX (SF3A1) related to RNA processing and a cell wall 1,2-ALPHA-FUCOSIDASE. REGULATORY PROTEIN SHOU4, involved in cell wall organization and located on chromosome V, was identified as a key sexual regulator. In contrast, Tak-2 showed proteins related to vesicle trafficking such as ARF-GTPASE GUANYL-NUCLEOTIDE EXCHANGE FACTOR (GBF) and GOLGIN (GC6) (Figure 4B), which showed direct interaction. GBF displayed numerous photosynthetic edges, as well as a COMPONENT MAC7 OF NON-SNRNP MOS4-ASSOCIATED COMPLEX (MAC7), involved in RNA processing. A-CLASS RAB GTPASE, related to vesicle trafficking and located in chromosome U, was a strong sexual regulator.

Following the highlighted proteins in Tak-1 distinction by previous analyses (Figure 4C; Table S4), cell wall MIK2 was found to be interacting with proteins implied in protein-/RNA-biosynthesis as well as phytohormone action. These proteins included TRANSLATION ELONGATION FACTOR (EF-Tu), COMPONENT MED12 OF KINASE MODULE OF MEDIATOR TRANSCRIPTION CO-ACTIVATOR COMPLEX (MED12) located on chromosome V and ALLENE OXIDASE CYCLASE (AOC). Moreover, the previously highlighted PP5 was linked strongly to cell wall regulation by MYO-INOSITOL-1-PHOSPHATE PHOSPHATASE (MIPP). Last, the PAO protein, which was described as distinctive for Tak-1, was connected to MIK2 by BETA-N-ACETYLHEXOSAMINIDASE (HEXO), a protein modification-related protein.

Regarding the previously highlighted proteins for Tak-2 distinction (Figure 4D; Table S4), FBL, NTF2 and GST were linked by a class PHI GLUTATHIONE *S*-TRANSFERASE (GSTF), which is related to redox homeostasis. FBL was connected to various lipid, photosynthetic and chromatin proteins such as PLASTIDIAL ACETYL-COA SYNTHETASE (ACS), A-CARBONIC ANHYDRASES (A-CAS) and HELICASE COMPONENT RVB (RVB), respectively. NTF2 interacted with a MAP-KINASE (NRK/MPK) as well as more redox proteins

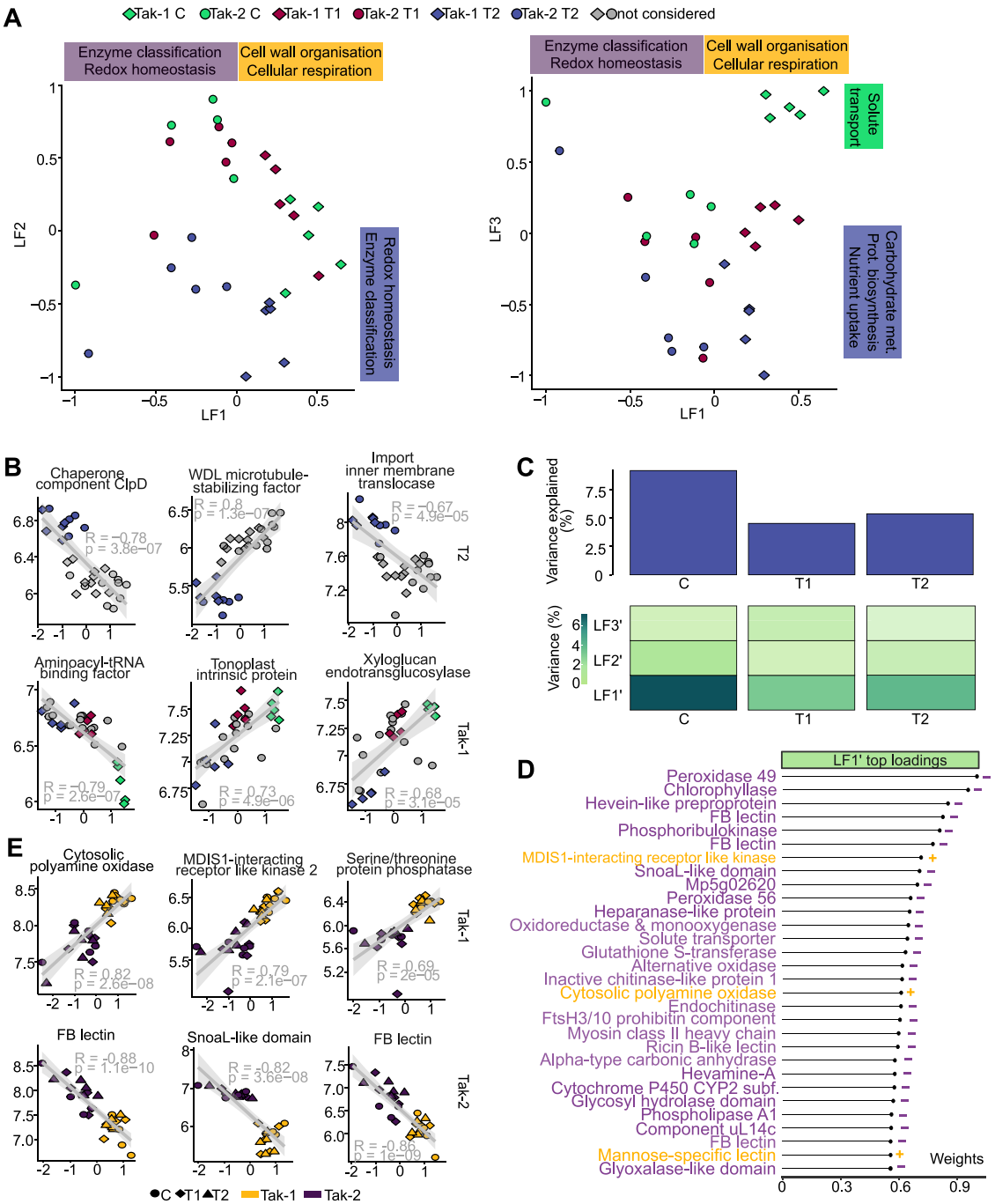

Figure 3. Latent factor analysis of proteomic data (Tak-1 and Tak-2 in C, T1, T2)

(A) Scatter plots from ungrouped analysis of latent factor 1 (LF1, *x*-axis) with latent factor 2 (LF2, *y*-axis) on the left side and latent factor 1 (LF1, *x*-axis) with latent factor 3 (LF3, *y*-axis) on the right side, illustrating variation described by each factor; samples are colored according to accessions (Tak-1 represented by circle figures, Tak-2 by diamond figures) and treatments (C in green, T1 in red, T2 in blue); MapMan enrichments are represented for accession differentiation (Tak-2 in purple square, and Tak-1 in yellow square at the top of each scatter plot), T2 differentiation (T2 in blue square on the left scatter plot) and specific Tak-1 differentiation (Tak-1 C in green square and Tak-2 T2 in blue square on the right scatter plot). **(B)** The specific representation of highlighted differentiation markers. The first row shows T2 markers, and the second row shows Tak-1 markers for each time (the remainder of the samples not considered in differentiation are shown in gray). **(C)** Percentage of explained variance (%) by each factor (rows) from grouped analysis across stress treatments (columns). **(D)** Lollipop plots showing top loadings of latent factor 1' (LF1') related to accession differentiation in all analyzed times by grouped analysis. Tak-2 loadings are represented in purple, and Tak-1 loadings are represented in yellow. **(E)** Specific representation of highlighted differentiation markers. The first row shows Tak-1 markers in yellow, and in the second row shows Tak-2 markers in purple. C as control and T1 and T2 as first and second daily combined stress intervals, respectively.

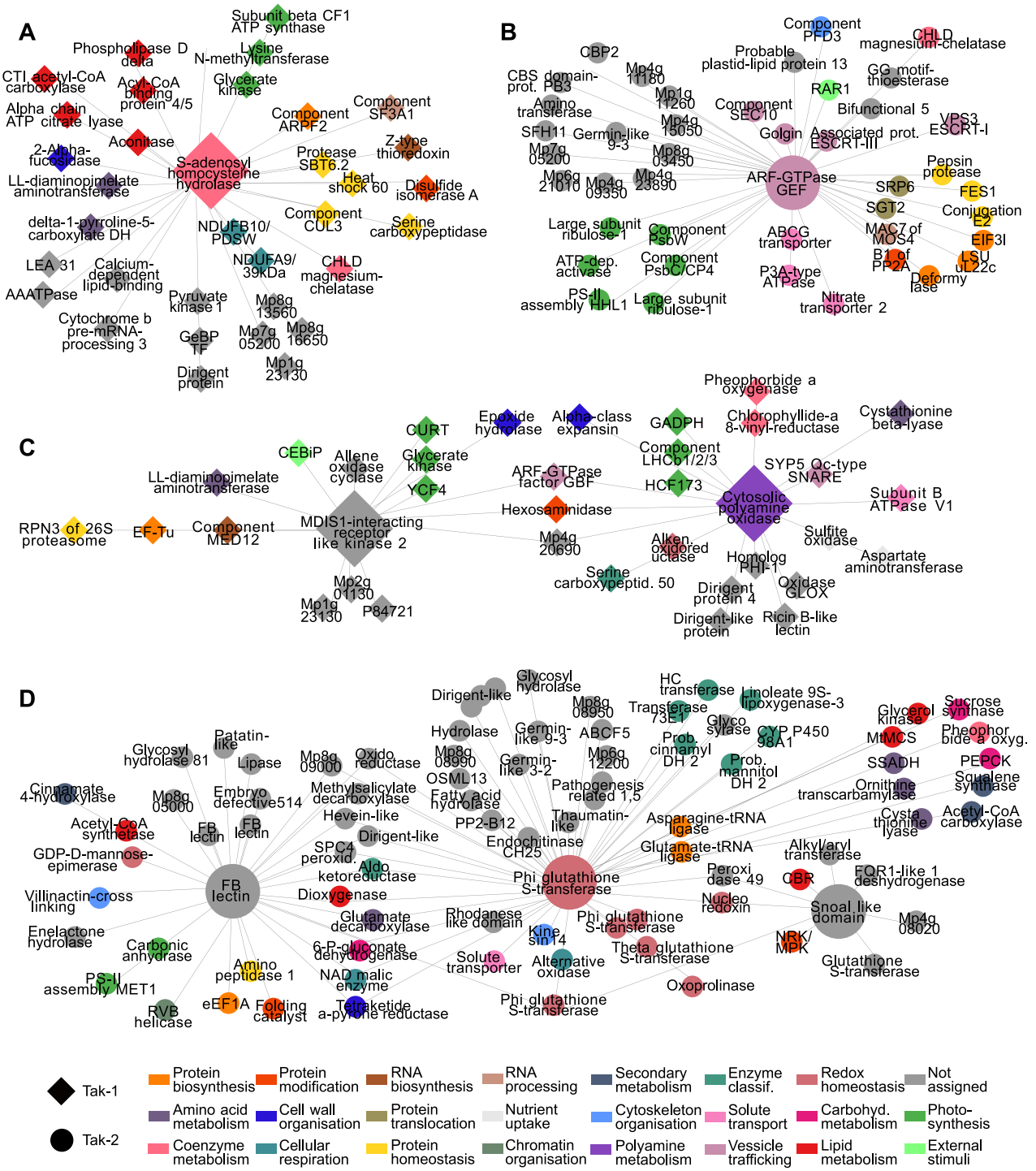

Figure 4. Meta-network analysis from proteomic data

(A) and **(B)** Strongest regulators interactions (by Katz centrality) from each Tak-1 (diamond symbols) and Tak-2 (circle symbols) meta-networks, respectively; proteins are annotated and colored by MapMan categories. **(C)** and **(D)** Top loading links for each Tak-1 (diamond symbols) and Tak-2 (circle symbols) meta-networks, respectively.

such as PEROXIDASE 49 (PX49), a previously potential marker for Tak-2, linking NTF2 and GST in the network. Redox homeostasis seemed to be a basal category only in Tak-2. The presence of the redox homeostasis category in network module 1 when stress machinery categories were under-accumulated supported this hypothesis.

Distinctive gene age trends for stress and sex protein sets were reported

The evolutionary context in which this species is situated prompted an evolutionary evaluation of proteomic data using Transcriptome Age Index (TAI) and phylostratum (PS) analyses. PS classification refers to a set of genes with the same

phylogenetic origin, ranging from PS1 related to cellular organism proteins to PS12 related to specific *M. polymorpha* proteins.

Differential TAI trends were observed across accessions and stress response (Figure 5A; Table S5). Tak-2 tended to accumulate younger proteins than Tak-1 under control and T1 conditions, with protein abundances of each PS equating at T2. Moreover, the stress times T1 and T2 presented younger proteomes compared to the control. The overall TAI profile significantly resembled the reductive hourglass pattern and early conservation pattern (low, high, high structure), which are common distributions observed in biological processes.

Comparing proteins associated with sex-biased phylostrata, (Figure 5B–D; Table S5), an abrupt association was showed, potentially relating their differences to booms in certain PS or specific origins in evolution. In contrast, comparing proteins associated with age-biased phylostrata (Figure 5B–D), it seemed that stress mechanisms were associated with a more continuous evolutionary gradient of PS complexity in both accessions, reinforcing the strong relationship of younger proteins with stress exposures.

The evaluation of sex and stress markers revealed differential trends across natural variation in *M. polymorpha*

Potential strong markers for stress and sex identity were identified. To explore the role of these proteins further, the gene expression of selected protein markers was analyzed in males (Tak-1) and females (Tak-2) from Japan, in males (Cam-1) and females (Cam-2) from the United Kingdom and in males (sAUS01) and females (sAUS02) from Australia, all subjected to same combined heat-drought stress experiment (see Materials and Methods).

F_v/F_m measurements revealed that Australian accessions (sAUS) exhibited stronger stress tolerance, particularly after longer stress exposure at T3, in contrast to accessions from the United Kingdom and Japan (Cam and Tak) which appeared to be more susceptible (Figures 6A, S3; Table S6).

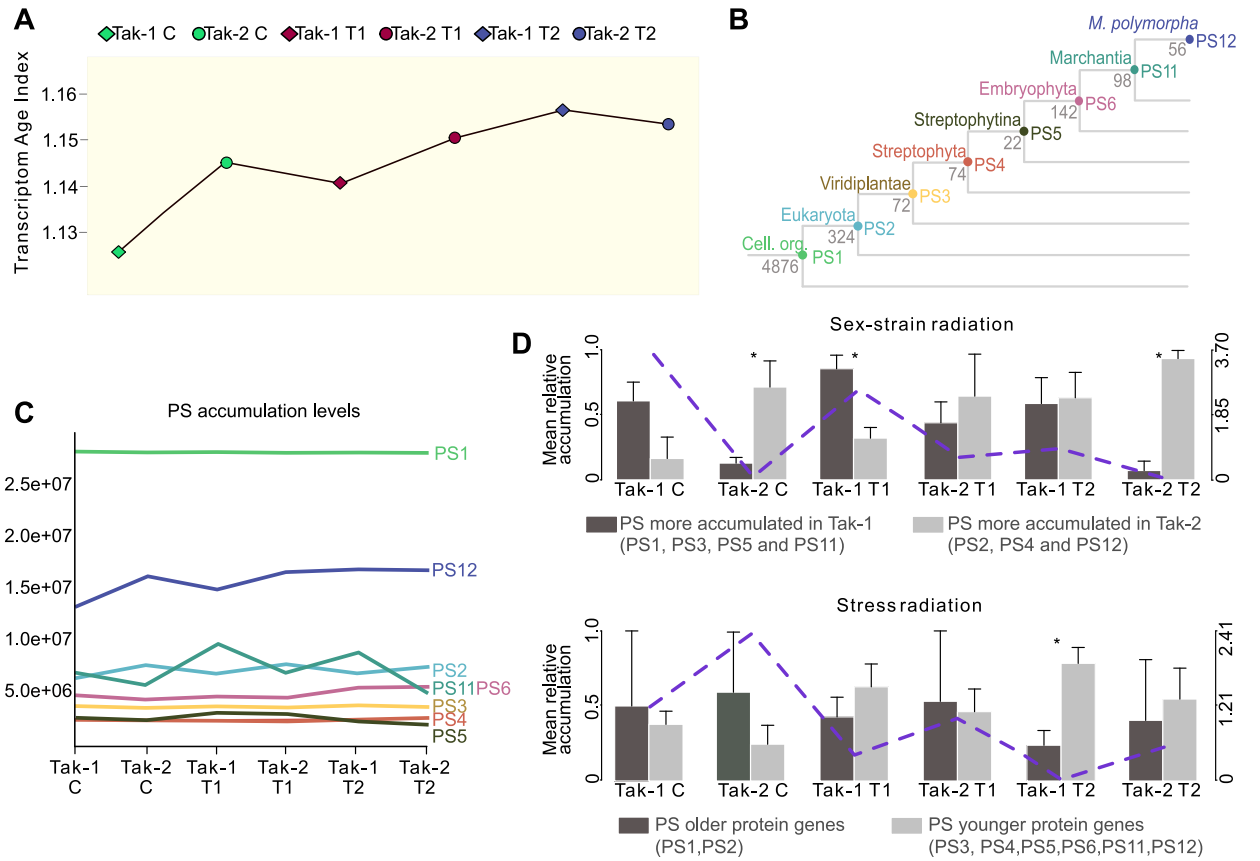

Figure 5. Evolutionary proteomics considering analyzed times (C, T1, and T2) and both accessions (Tak-1 and Tak-2)
(A) Transcriptome Age Index (TAI) corresponding high values to younger protein genes. **(B)** Phylostratum (PS) classification on this species. **(C)** Protein gene abundance for each phylostratum (PS) accumulation level. **(D)** PS tendencies comparing at the top graphic, PS tendentially more accumulated on Tak-1 (PS1, PS3, PS5, and PS11, black bars) versus PS tendentially more accumulated on Tak-2 (PS2, PS4, and PS12, gray bars) and at the bottom graphic, old protein genes (PS1 and PS2 black bars) versus young protein genes (rest PS, gray bars) in the different biological sets; PS abundances are represented on bars corresponding to left axis scale and relative abundances between both groups on a biological set are represented on discontinuous blue line corresponding to right axis scale. Asterisks (*) denote significant differences among treatments ($P < 0.05$). C is the control and T1 and T2 are the first and second daily combined stress intervals, respectively.

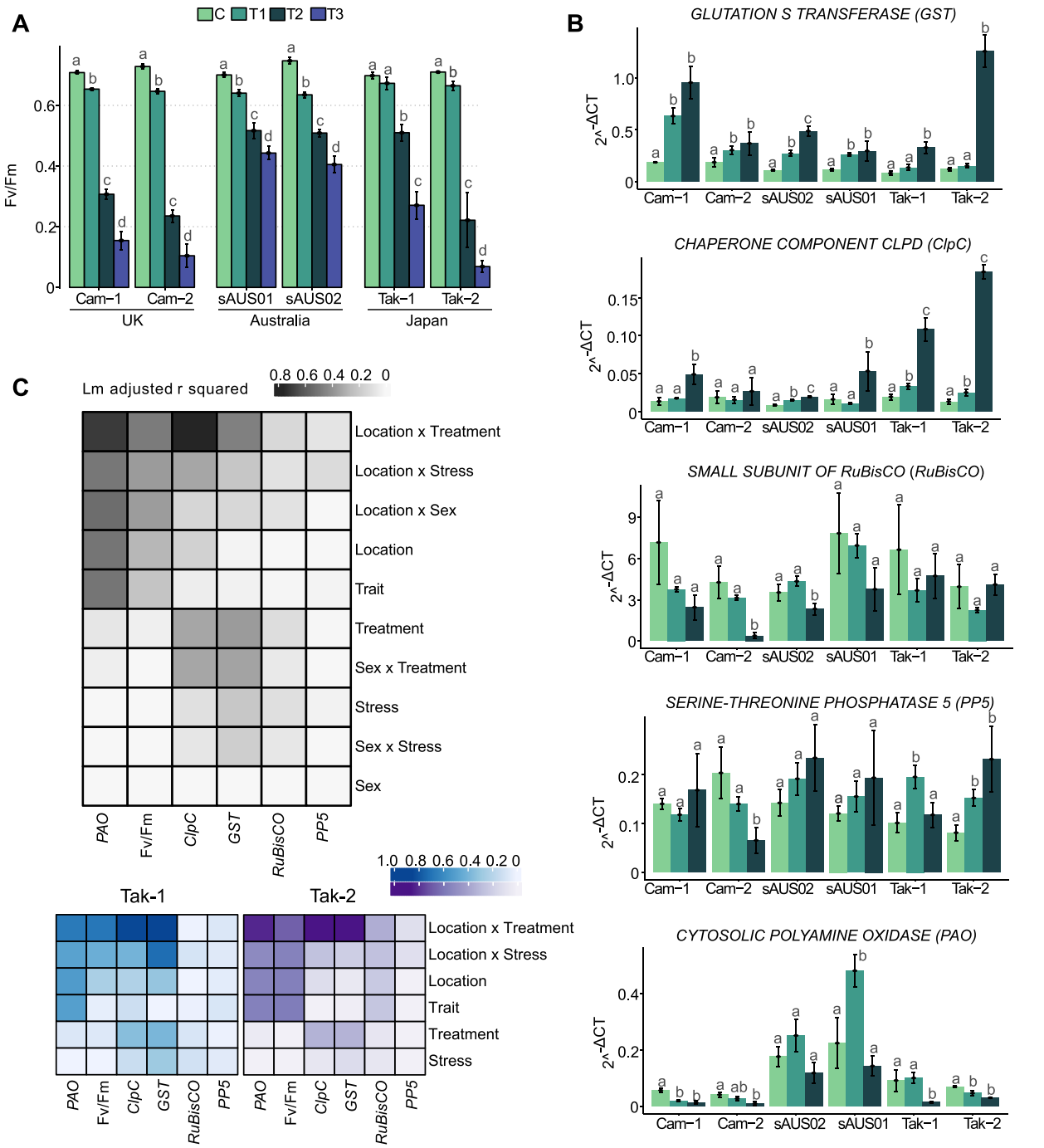

Figure 6. Complementary protein analyses from a natural variation perspective

(A) and **(B)** Evaluation of different natural accessions (Cam-1 and Cam-2, Tak-1 and Tak-2, sAUS01 and sAUS02) to combined heat and drought stress, representing maximal efficiency of photosystem II (F_v/F_m) and gene expression of selected markers, respectively; different letters indicate significant differences comparing each accession stress responses ($P < 0.05$). **(C)** Linear regression heatmaps with colors indicating explained variance; gray heatmap with global data, blue heatmap with Tak-1 data and purple heatmap with Tak-2 data.

Different trends in marker gene expression were established, distinguishing accessions based on their stress response, local origin or sexual genotype. Stress-related genes such as *GLUTATHIONE S-TRANSFERASE* (*GST*) and *CHAPERONE COMPONENT CLPD OF CHLOROPLAST CLP-TYPE PROTEASE COMPLEX* (*ClpC*) showed similar patterns across all accessions, being upregulated under stress conditions, especially at T2 (Figure 6B; Table S6). Furthermore, the *SMALL SUBUNIT OF RIBULOSE-1,5-BISPHOSPHAT CARBOXYLASE/OXYGENASE HETERODIMER* (*RuBisCO*) showed varying tendencies among pairs of accessions from different locations but similar behavior within male and female. Cam and Tak accessions downregulated this gene at T1, unlike the almost unchanged expression observed in sAUS accessions.

Conversely, *PP5 SERINE-THREONINE PHOSPHATASE (PP5)* showed differing trends within the same pair of accessions (male and female), only in the more susceptible ones (Cam and Tak) (Figure 6B; Table S6). Finally, *CYTOSOLIC POLYAMINE OXIDASE (PAO)* displayed distinct behaviors between susceptible and tolerant accessions, with expression levels notably higher in the more tolerant accessions (sAUS), under control and in stress conditions (Figure 6B; Table S6).

To evaluate the variability between sexes and location sites, linear regression models were constructed to elucidate gene expression and photosynthetic changes during our assay, comparing location (Australia, Japan, and the United Kingdom), treatment (C, T1, and T2), stress (control and stress), sex (male and female) and trait (tolerant and susceptible) as factors along with their interactions (Figure 6C). Generally, treatment and its interaction with location emerged as good predictors of *GST* and *ClpC* expression. Moreover, location was identified as a good predictor of *PAO* expression. Notably, changes in expression were barely predicted by sex. Consequently, linear regression models were recomputed independently for each sex. While *GST* expression was predicted by stress only in males, females required additional information. However, photosynthetic-related features (F_v/F_m and *RuBisCO*) in females were strongly influenced by location, in contrast to males.

DISCUSSION

Marchantia polymorpha is a prominent species for climate change studies, having adapted to terrestrial stressors and extreme aerial conditions over 400 million years ago. Its dioicous behavior can lead to differences in energetic priorities and, consequently, varying survival outcomes due to stress, which may limit the species' perpetuation. In this study, employing a systems biology approach, we successfully established global and specific overviews of response cascade and sexual identity. This allowed us to identify mechanisms involved in the stress distinction between sexual accessions, shedding light on a potential evolutionary flux of key events in plant history, such as sexual divergence and stress radiation.

Overall stress responses were similar between sexual accessions (Figure 7). Combined heat and drought stress led

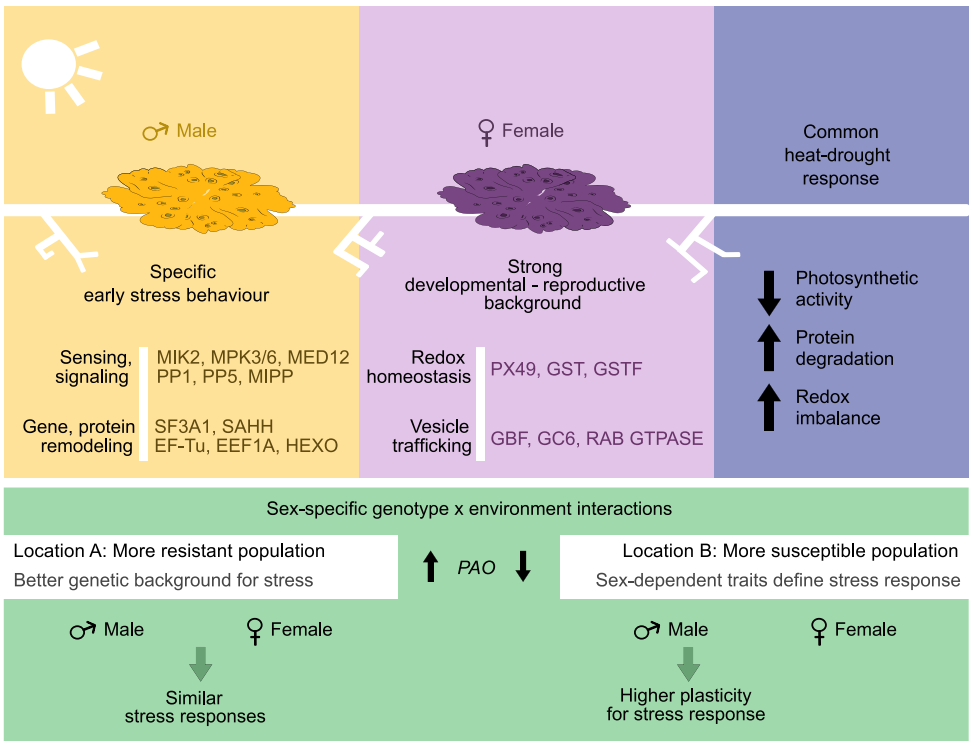

Figure 7. Overview of highlighted mechanisms involved in combined heat and drought responses and potential hypothesis for the differential behavior between sexual accessions (male and female)
The top panel presents an overview of unique and common stress dynamics among accessions through the proteomic layer (arrows indicate a functional decrease or increase in response to stress). The bottom panel proposes a hypothesis for the sex-dependent stress response linked to local adaptation (arrows in *PAO* indicate its increase or decrease in more resistant or susceptible accessions, respectively). EEF1A: AMINOACYL-TRNA BINDING FACTOR; EF-Tu: TRANSLATION ELONGATION FACTOR; GBF: ARF-GTPASE GUANYL-NUCLEOTIDE EXCHANGE FACTOR; GC6: GOLGIN; GST: GLUTATHIONE S-TRANSFERASE; GSTF: PHI GLUTATHIONE S-TRANSFERASE; HEXO: BETA-N-ACETYLHEXOSAMINIDASE; MED12: COMPONENT MED12 OF KINASE MODULE OF MEDIATOR TRANSCRIPTION CO-ACTIVATOR COMPLEX; MIK2: LEUCINE-RICH REPEAT MDIS1-INTERACTING RECEPTOR-LIKE KINASE 2; MIPP: MYO-INOSITOL-1-PHOSPHATE PHOSPHATASE; MPK3/6: MAPK KINASE 3/6; PAO: CYTOSOLIC POLYAMINE OXIDASE; PP1: SERINE/THREONINE PROTEIN PHOSPHATASE; PP5: PP5 PHOSPHATASE; PX49: PEROXIDASE 49; SAHH: *S*-ADENOSYL HOMOCYSTEINE HYDROLASE; SF3A1: COMPONENT SF3A1 OF SPLICING FACTOR 3A COMPLEX.

to an irreparable decrease in photosynthetic activity, an increase in protein degradation and a redox imbalance (Albert et al., 2018; Ghosh et al., 2021). Similar responses between sexual accessions were observed, especially at longer stress exposures, where proteins were coded by genes that are more recent in evolutionary time. As a key species in terrestrial adaptation, many of its specific genes (evolutionarily younger) are likely to be linked to stress responses due to fitness benefits, as previously suggested in yeasts (Doughty et al., 2020).

However, male Tak-1 showed a specific early behavior that led to different stress adjustment timings, remarking a higher susceptibility in female Tak-2 (Figure 7). Tak-2 individuals were indeed capable of sensing the first pulse of stress but seemed to lack the mechanisms needed for a quicker response, thus experimenting with a stronger shock. This early stress differentiation of Tak-1 could be related to distinctive sensing and signaling. Numerous kinases, such as MIK2 and MPK3/6, could be interplaying in gene and protein networks, facilitating faster gene regulation by splicing (SF3A1), epigenetics (SAHH) and translation remodeling (EF-Tu) (Van Der Does et al., 2017). A drought experiment on *Marchantia inflexa* suggested that transcriptional differences contributed to the observed stress variation among sexual and tissue genotypes (Marks et al., 2021). Highlighted phytocompound metabolisms such as abscisic acid (ABA) (Tougane et al., 2010; Arias et al., 2018) and polyamines (Smith and Maravolo, 2004) could be directly or indirectly influencing the acclimation process by cytosolic polyamine oxidases (PAO) and phosphatases (PP1) and malic enzymes (NADP-ME), respectively. ABA is recognized as a master regulator in land plant evolution (Eklund et al., 2018; Wu et al., 2022b). It is linked to late embryogenesis abundant proteins highlighted in this stress response (LEA14), which regulate protein homeostasis, membrane integrity and photosynthesis (Liang et al., 2019). Despite this species presenting an evolutionary gene loss of stomata (Clark, 2023), the highlighting of ABA signaling components in this experiment links its ancestral function to stress responses independently from stomata presence. Moreover, it is also known that different polyamines are required for growth and stress responses in this species (Furumoto et al., 2024), being related to transcription factors involved in redox processes (Busch et al., 2019). Altogether it underscores the important role of phytohormones in terrestrial invasion, potentially interacting with each other as demonstrated in other model species (Wimalasekera et al., 2015).

The female genetic background appeared to be primarily focused on reproductive traits. Female Tak-2 identity was associated with redox and vesicle trafficking with various peroxidases (PX49), glutathione transferases (GST) and GTPases (RAB and GBF), being functional categories highlighted in female development and reproduction (Martin et al., 2013; Rojek et al., 2021). During stress recovery, females Tak-2 prioritized the quality of offspring over quantity, contrasting with males Tak-1 (McLetchie and Puterbaugh, 2000). Furthermore, female reproductive structures are essential for the development of sexual spores and the perpetuation of the species (Bowman et al., 2022). Previous experiments in other species have evidenced lower stress tolerances in female individuals, partially attributed to this greater reproductive cost (Juvany and Munné-Bosch, 2015).

Sex-dependent stress behaviors seemed to be strongly linked to local adaptation traits (Figure 7). Natural populations of *M. polymorpha* exhibited varying tolerances to combined heat-drought stress. For instance, natural variation processes may be affecting polyamine genes (*PAO*) in this basal species, as shown in more recent ones, resulting in different degrees of stress tolerance (Fujita et al., 2012). Most of their variability was related to the populations' geographical origin rather than sexual identity, likely due to extensive gene exchange within populations. However, more susceptible populations showed marked differences between sexual accessions, contrary to resistant population trends. This was exemplified by *PP5*, which displayed sex differences in susceptible accessions and has been linked to thermotolerance and retrograde signaling in certain model species, among other functions (Park et al., 2011; Barajas-López et al., 2013). Local adaptation and genotypic diversity could be driven by sex-specific genotype environment interactions (Healey et al., 2023). Female and male accessions from a more resistant population may present a better genetic background to respond to stress, thereby avoiding sex-dependent compromises. However, as stress pressure intensifies in susceptible populations, sexual traits occur that define and differentiate the stress response, with male Tak-1 exhibiting greater plasticity towards it. Our findings suggest that female accession could have lost stress plastic mechanisms for the benefit of stability and reproductive success, whereas male accession could have retained them as adaptive traits for dispersal and mobility-related functions (Bowman et al., 2022). Sex-biased traits frequently rely on interactions between autosomal and sexual genes (Healey et al., 2023). The female Tak-2 accession showed a younger proteome than male Tak-1, potentially reinforcing the idea of an active induction of female identity as opposed to a default male identity (Hisanaga et al., 2019; Iwasaki et al., 2021). This intriguing topic has already been approached in fungi, where gene age seems to module transcriptional changes on sexual processes (Merényi et al., 2022).

A variety of biological factors, including stage of development, type of tissue, environmental location and sexual variation may concurrently influence the stress response. Our hypothesis supports the idea that sex-specific plasticity is essential for modeling combined heat and drought responses when local adaptation traits constrain plant survival. In future research, it will be valuable to delve deeper into natural variation and stress processes more representatively, considering more environmentally diverse populations, conducting functional validation and investigating potential effects of stress memory.

MATERIALS AND METHODS

Plant material and experimental design

Gemmae from Tak-1 (Takaragaike-1, male accession) and Tak-2 (Takaragaike-2, female accession) from *M. polymorpha* were cultivated on half-strength Gamborg's B5 medium containing 1% agar (w/v) at 21°C under long-day conditions (16 h light/8 h dark) with 80 μmol m^{-2} s^{-1} light (PAR) for 15 d. Subsequently, for a natural response experiment, mature thalli were transferred to ex vitro conditions on peat:perlite (3:1) plates on a Fitoclima 1200 climate chamber (Aralab; Albarraque, Portugal) under long-day conditions, with 50%–60% relative humidity (RH), for approximately 15 d until complete thalli re-acclimation.

A combined heat-drought stress assay was performed on 1-month-old thalli maintaining previous temperature and photoperiod conditions except from combined stress periods. This was conducted using a controlled Fitoclima 1200 climate chamber (Aralab; Albarraque, Portugal). Heat stress involved daily shocks at noon (12:00 h) with a gradual temperature increase (15-min ramp) to 27°C stress temperature, maintained for 1 h, followed by a gradual temperature descent to 21°C culture temperature (15-min ramp). Drought stress by suspending irrigation began with the first heat shock and was progressive over time, resulting in approximately 15% SWC substrate loss per day. Plants were irrigated to field capacity at control conditions, establishing this SWC as 100%. To investigate various regulation points of the stress response, we optimized stress conditions to cover different response times. As a result, different treatment intervals were measured and sampled: before the first heat shock (control, C) and after first (T1, first day), second (T2, second day) and third (T3, third day) daily combined stress intervals (heat shocks plus progressive drought). Therefore, stress treatments were applied for three consecutive days, resulting in a total substrate of 45% SWC by the end of the stress experiment. A parallel control was not conducted daily due to the short duration of the experiment, during which potential developmental changes were deemed unlikely to significantly impact the results. Thalli were rapidly fast-frozen in liquid nitrogen and stored at −80°C until biochemical and proteomic procedures were carried out. Five biological replicates per treatment (C, T1, T2, T3) and accession (Tak-1 and Tak-2) were established, coming from different biological lines. All samples were grown simultaneously and evaluated in the same stress experiment.

Photosynthetic measurements and physiological markers quantification

To assess stress-induced damage to the photosynthetic process, chlorophyll fluorescence was measured at the conclusion of each treatment interval (C, T1, T2, T3), around 1 h and a half after noon, using a OS1p-FL chlorophyll fluorometer (Opti-Sciences; Hudson, USA). To determine the maximum quantum efficiency of photosystem II (PSII) (F_v/F_m), thalli were subjected to dark conditions for 20 min prior to measurement and then applied a short pulse of saturating light (0.8 s at 8,000 μmol photons m^{-2} s^{-1}). Pre-established criteria were followed for the calculation of photosynthetic parameters (Maxwell and Johnson, 2000).

The physiological evaluation of Tak-1 and Tak-2 was conducted at treatment times C, T1 and T2, as the T3 period was associated with senescence processes due to significantly reduced photosynthetic activity (F_v/F_m). The extraction and quantification of molecular metabolism markers (chlorophylls *a* and *b*, carotenoids, free amino acids, total phenolic compounds, and MDA) were performed according to López-Hidalgo et al. (2021). This protocol began with 10 mg of dry and homogenized thalli and extraction was carried out using ethanol.

The statistical evaluation of these measurements was carried out in R programming language (v.4.1.2) running under RStudio (version 2021.09.2 + 382) employing the *agricolae* package (v.1.3-5) (https://cran.r-project.org/package=agricolae). For parametric variables, one-way ANOVA with post-hoc Tukey HSD was carried out and for non-parametric variables, Kruskal–Wallis with post-hoc Dunn test (P-value < 0.05).

Protein purification, identification and quantitation (nLC-Orbitrap/MS)

The proteomic evaluation was performed on C, T1 and T2 treatment times, as T3 was related to senescence processes as detailed above.

Proteins were extracted using 20 mg of lyophilized weight per sample (Valledor et al., 2014a) with phenol (Tris-buffered pH 8) and water, precipitated by 0.1 M ammonium acetate in methanol with 0.5% β-mercaptoethanol, rehydrated in 8 M urea and 4% SDS and quantified with bicinchoninic acid (BCA) method. Subsequently, 60 μg of proteins were in-gel cleaned, digested with trypsin (Roche) and desalted following the Valledor and Weckwerth protocol (2014). Peptides were analyzed on an nLC-Orbitrap Lumos/MS system (Thermo Fisher; Vienna, Austria) employing an 85 min gradient and a 150 mm length RP-C18 column (Zorbax) following a top30 approach for peptide selection.

Proteome Discoverer 2.0 (Thermo Fisher; USA) and SEQUEST algorithm were employed for peptide processing and protein identification and quantitation, establishing at least one high-confidence unique peptide umbral for protein identification and one peptide (unique/razor) per protein for label-free quantification (FDR threshold, q-value of 0.01). Two databases were employed for identification: *Marchantia polymorpha* (Phytozome v.3.1) and Viridiplantae (UniProt reviewed 20211230 version). Consequently, out of a total of 5,869 detected and identified proteins, 4,001 were classified as high-confidence proteins (68.2% of the total identified proteins). Proteins were annotated according to MapMan functional categories (Bins) using Mercator4 (v.2.0).

Proteomic analysis

Descriptive proteomics

Descriptive analyses were performed using the *pRocessomics* R package (v.0.1.13, github.com/Valledor/pRocessomics) developed in our laboratory group, following the recommendations of Valledor et al. (2014b) for imputation, abundance

balancing normalization and data pre-filtering. Briefly, missing values and one of five replicates from the control male were imputed using the random forest (RF) method, with an imputation threshold of 20% on each treatment. Variables present in <45% of total samples were excluded from the analysis. Therefore, out of a total of 4001 high-confidence proteins, 3,577 proteins met these pre-established criteria (61% of total identified proteins). Abundances were normalized using a sample-centric approach and multiplied by the average intensity of all samples. Univariate analyses (non-parametric Kruskal–Wallis with post-hoc Dunn test), Venn diagrams (variables present in four of five biological replicates of treatment were considered), heatmaps (constructed by mean of all biological replicates, for further information from all replicates independently see Table S2) and hierarchical clustering and *K*-means clustering (confidence interval of 95%) and its MapMan functional enrichments (*P*-value threshold 0.05) using the *gprofiler2* package (v.0.2.1) were performed within this package.

Identification of latent sources of variation

Inference of sources of variation was performed in R using the MOFA2 package (v.1.0.1) (Argelaguet et al., 2020), selecting the top 2,000 features with the highest variance with a log10 + 10 transformation for the analysis. Initially, an ungrouped framework for general sources of variation was employed, followed by a multi-group framework establishing treatment times (C, T1, and T2) as supervised groups. Model training was performed using maxiter = 100,000 and convergence_mode = "slow." Mercator4 MapMan functional enrichments of latent factors were subsequently performed.

Meta-network analysis

A meta-network was generated for each accession as a consensus of various mathematical algorithms using the Seidr network toolkit (v.0.14.2) (Schiffthaler et al., 2023). To control bias by specific type of protein interactions ARACNE, CLR, Spearman correlation, Elastic Net and SVM ensemble methods, GENIE3, NARROMI, Partial Correlation, PLSNET, TIGRESS and TOM similarity inference methods were applied. Proteomic data were transformed by log10 + 10 and were centered around the median for the analysis. Individual networks converged into a meta-network using the "irp" method, and the resultant meta-network was filtered by network backboning with -F 1.28. Infomap (v.1.3.0) was utilized to identify highly connected protein modules and *The Neat* (v.1.1.3) R package (https://cran.r-project.org/package=neat) was used to analyze module enrichments using Mercator4 MapMan functional categories ($\alpha = 0.05$).

Evolutionary proteomics

To classify proteomic information in categories based on phylogenetic origin- and diversity- patterns, the myTAI R package (v.0.9.3) (Drost et al., 2018) was used, alongside a quantile transformation of protein data. Phylostratum (PS) information, which classifies genes according to phylogenetic origins, was obtained using genEra software (v.1.0.2). The database was completed by adding gymnosperms data due to their little representation on NCBI (*Pinus taeda* and *Ginkgo biloba* information from https://treegenesdb.orgdatabase). The TAI approach for gene age evaluation was followed in various analyses, including the Flat Line Test, Reductive Hourglass, Reductive Early Conservation and Reverse Hourglass Tests (Early module conformed by controls, Mid module by T1 and Late module by T2).

Evaluation of stress and sex proteomic markers by targeted transcriptomics

An additional stress experiment following the same conditions and design was conducted in additional natural accessions from this species: Tak-1 (male) and Tak-2 (female) from Japan, Cam-1 (Cambridge-1, male) and Cam-2 (Cambridge-2, female) from the United Kingdom and sAUS01 (male) and sAUS02 (female) from Australia.

Chlorophyll fluorescence was measured throughout the experiment according to the aforementioned protocol. To evaluate the expression of selected potential protein markers, total RNA was extracted at C, T1, and T2 following the method described by Valledor et al. (2014a). RNA concentration was determined using a Nabi UV/Vis Nano Spectrophotometer and its integrity was checked using agarose gel electrophoresis. Next, cDNA was synthesized using the RevertAid kit (ThermoFisher Scientific) with random hexamers as primers following the manufacturer's instructions. qPCR analyses were carried out by a CFX96™ Real-Time System (Bio-Rad; Hercules, USA) using the BlasTaq™ 2X qPCR MasterMix (Applied Biological Materials; Vancouver, Canada). The results were analyzed using the cycle threshold comparative method (CT). Each treatment included three biological and two analytical replicates. *ACTIN 7* (*MpACT*) was used as a reference gene for normalizing transcript levels. Statistical evaluation of photosynthetic and qPCR results was carried out comparing each accession stress response (C, T1, T2), as described previously. Linear regression models for predicting expression and photosynthetic changes by design factors (location: Australia, Japan and the United Kingdom; treatment: C, T1, and T2; stress: control and stress; sex: male and female; trait: tolerant and susceptible) along with their interactions were performed using the "lm" function in the *stats* R package (v.4.3.3).

Data availability statement

All data and code generated during this study are available in the GitHub repository (https://github.com/Valledor/HxD_Marpol_Proteomics). The mass spectrometry proteomics data have been deposited to the ProteomeXchange Consortium via the PRIDE partner repository (Perez-Riverol et al., 2022) with the dataset identifier PXD047874 (https://www.ebi.ac.uk/pride/archive/projects/PXD047874).

ACKNOWLEDGEMENTS

We extend our gratitude to Roberto Solano, John Bowman and Jim Haseloff for generously providing Marchantia

accessions. This work was funded by the Spanish Ministry of Science, Innovation and Universities (PID2020-113896GB-I00). Sara Guerrero and Lara García-Campa are supported by Severo Ochoa Predoctoral Program (BP19-145 and BP19-146, respectively) from Government of Principado de Asturias (Spain). Víctor Roces is supported by FPU fellowship program from the Spanish Ministry of Universities (FPU18/02953).

CONFLICTS OF INTEREST

The authors declare there is no conflict of interest.

AUTHOR CONTRIBUTIONS

S.G. and M.M. conceived and designed the study. S.G., L.G.-C., and V.R. performed the experiments. S.G. and L.V. performed proteomic analysis. S.G. and V.R. concluded computational analyses. M.M. and L.V. supervised the study. S.G. and M.M. wrote the manuscript. All authors revised and approved the final manuscript draft.

Edited by: Martin Parry, Lancaster University, UK

Received Jan. 15, 2024; **Accepted** Jul. 11, 2024; **Published** Aug. 7, 2024

OO: OnlineOpen

REFERENCES

Akter, K., Kato, M., Sato, Y., Kaneko, Y., and Takezawa, D. (2014). Abscisic acid-induced rearrangement of intracellular structures associated with freezing and desiccation stress tolerance in the liverwort *Marchantia polymorpha*. J. Plant Physiol. **171:** 1334–1343.

Albert, N.W., Thrimawithana, A.H., McGhie, T.K., Clayton, W.A., Deroles, S.C., Schwinn, K.E., Bowman, J.L., Jordan, B.R., and Davies, K.M. (2018). Genetic analysis of the liverwort *Marchantia polymorpha* reveals that R2R3MYB activation of flavonoid production in response to abiotic stress is an ancient character in land plants. New Phytol. **218:** 554–566.

Argelaguet, R., Arnol, D., Bredikhin, D., Deloro, Y., Velten, B., Marioni, J.C., and Stegle, O. (2020). MOFA+: A statistical framework for comprehensive integration of multi-modal single-cell data. Genome Biol. **21:** 111.

Arias, C.L., Pavlovic, T., Torcolese, G., Badia, M.B., Gismondi, M., Maurino, V.G., Andreo, C.S., Drincovich, M.F., Gerrard Wheeler, M.C., and Saigo, M. (2018). NADP-dependent malic enzyme 1 participates in the abscisic acid response in *Arabidopsis thaliana*. Front. Plant Sci. **9:** 1637.

Barajas-López, J.D.D., Kremnev, D., Shaikhali, J., Piñas-Fernández, A., and Strand, Å. (2013). PAPP5 is involved in the tetrapyrrole mediated plastid signalling during chloroplast development. PLoS One **8:** e60305.

Bigot, S., Buges, J., Gilly, L., Jacques, C., Le Boulch, P., Berger, M., Delcros, P., Domergue, J., Koehl, A., Ley-Ngardigal, B., et al. (2018). Pivotal roles of environmental sensing and signaling mechanisms in plant responses to climate change. Glob. Chang. Biol. **24:** 5573–5589.

Bowman, J.L., Kohchi, T., Yamato, K.T., Jenkins, J., Shu, S., Ishizaki, K., Yamaoka, S., Nishihama, R., Nakamura, Y., Berger, F. et al. (2017). Insights into land plant evolution garnered from the *Marchantia polymorpha* genome. Cell **171:** 287–304.e15.

Bowman, J.L., Arteaga-Vazquez, M., Berger, F., Briginshaw, L.N., Carella, P., Aguilar-Cruz, A., Davies, K.M., Dierschke, T., Dolan, L., Dorantes-Acosta, A.E., et al. (2022). The renaissance and enlightenment of *Marchantia* as a model system. Plant Cell **34:** 3512–3542.

Busch, A., Deckena, M., Almeida-Trapp, M., Kopischke, S., Kock, C., Schüssler, E., Tsiantis, M., Mithöfer, A., and Zachgo, S. (2019). *MpTCP 1* controls cell proliferation and redox processes in *Marchantia polymorpha*. New Phytol. **224:** 1627–1641.

Carella, P., Gogleva, A., Hoey, D.J., Bridgen, A.J., Stolze, S.C., Nakagami, H., and Schornack, S. (2019). Conserved biochemical defenses underpin host responses to oomycete infection in an early-divergent land plant lineage. Curr. Biol. **29:** 2282–2294.e5.

Clark, J.W. (2023). Genome evolution in plants and the origins of innovation. New Phytol. **240:** 2204–2209.

Clark, J.W., Hetherington, A.J., Morris, J.L., Pressel, S., Duckett, J.G., Puttick, M.N., Schneider, H., Kenrick, P., Wellman, C.H., and Donoghue, P.C.J. (2023). Evolution of phenotypic disparity in the plant kingdom. Nat. Plants **9:** 1618–1626.

Doughty, T.W., Domenzain, I., Millan-Oropeza, A., Montini, N., De Groot, P.A., Pereira, R., Nielsen, J., Henry, C., Daran, J-MG., Siewers, V., et al. (2020). Stress-induced expression is enriched for evolutionarily young genes in diverse budding yeasts. Nat. Commun. **11:** 2144.

Drost, H.-G., Gabel, A., Liu, J., Quint, M., and Grosse, I. (2018). myTAI: Evolutionary transcriptomics with R. Bioinformatics **34:** 1589–1590.

Eklund, D.M., Kanei, M., Flores-Sandoval, E., Ishizaki, K., Nishihama, R., Kohchi, T., Lagercrantz, U., Bhalerao, R.P., Sakata, Y., and Bowman, J.L. (2018). An evolutionarily conserved abscisic acid signaling pathway regulates dormancy in the liverwort *Marchantia polymorpha*. Curr. Biol. **28:** 3691–3699.e3.

Fujita, M., Fujita, Y., Iuchi, S., Yamada, K., Kobayashi, Y., Urano, K., Kobayashi, M., Yamaguchi-Shinozaki, K., and Shinozaki, K. (2012). Natural variation in a polyamine transporter determines paraquat tolerance in Arabidopsis. Proc. Natl. Acad. Sci. U. S. A **109:** 6343–6347.

Furumoto, T., Yamaoka, S., Kohchi, T., Motose, H., and Takahashi, T. (2024). Thermospermine is an evolutionarily ancestral phytohormone required for organ development and stress responses in *Marchantia polymorpha*. Plant Cell Physiol. **65:** 460–471.

Ghosh, T.K., Tompa, N.H., Rahman, Md.M., Mohi-Ud-Din, M., Al-Meraj, S.M.Z., Biswas, Md.S., and Mostofa, M.G. (2021). Acclimation of liverwort *Marchantia polymorpha* to physiological drought reveals important roles of antioxidant enzymes, proline and abscisic acid in land plant adaptation to osmotic stress. PeerJ **9:** e12419.

Hatchett, W.J., Jueterbock, A.O., Kopp, M., Coyer, J.A., Coelho, S.M., Hoarau, G., and Lipinska, A.P. (2023). Evolutionary dynamics of sex-biased gene expression in a young XY system: Insights from the brown alga genus *Fucus*. New Phytol. **238:** 422–437.

Healey, A.L., Piatkowski, B., Lovell, J.T., Sreedasyam, A., Carey, S.B., Mamidi, S., Shu, S., Plott, C., Jenkins, J., Lawrence, T., et al. (2023). Newly identified sex chromosomes in the *Sphagnum* (peat moss) genome alter carbon sequestration and ecosystem dynamics. Nat. Plants **9:** 238–254.

Hisanaga, T., Yamaoka, S., Kawashima, T., Higo, A., Nakajima, K., Araki, T., Kohchi, T., and Berger, F. (2019). Building new insights in plant gametogenesis from an evolutionary perspective. Nat. Plants **5:** 663–669.

Iwasaki, M., Kajiwara, T., Yasui, Y., Yoshitake, Y., Miyazaki, M., Kawamura, S., Suetsugu, N., Nishihama, R., Yamaoka, S., Wanke, D., et al. (2021). Identification of the sex-determining factor in the liverwort *Marchantia polymorpha* reveals unique evolution of sex chromosomes in a haploid system. Curr. Biol. **31:** 5522–5532.e7.

Juvany, M., and Munné-Bosch, S. (2015). Sex-related differences in stress tolerance in dioecious plants: A critical appraisal in a physiological context. J. Exp. Bot. **66:** 6083–6092.

Kosová, K., Vítámvás, P., Prášil, I.T., and Renaut, J. (2011). Plant proteome changes under abiotic stress—Contribution of proteomics studies to understanding plant stress response. J. Proteomics **74:** 1301–1322.

Liang, Y., Kang, K., Gan, L., Ning, S., Xiong, J., Song, S., Xi, L., Lai, S., Yin, Y., Gu, J., et al. (2019). Drought-responsive genes, late embryogenesis abundant group3 (*LEA 3*) and vicinal oxygen chelate, function in lipid accumulation in *Brassica napus* and *Arabidopsis* mainly via enhancing photosynthetic efficiency and reducing ROS. Plant Biotechnol. J. **17:** 2123–2142.

López-Hidalgo, C., Meijón, M., Lamelas, L., and Valledor, L. (2021). The rainbow protocol: A sequential method for quantifying pigments, sugars, free amino acids, phenolics, flavonoids and MDA from a small amount of sample. Plant Cell Environ. **44:** 1977–1986.

Marchetti, F., Cainzos, M., Cascallares, M., Distéfano, A.M., Setzes, N., López, G.A., Zabaleta, E., and Pagnussat, G.C. (2021). Heat stress in *Marchantia polymorpha*: Sensing and mechanisms underlying a dynamic response. Plant Cell Environ. **44:** 2134–2149.

Marks, R.A., Smith, J.J., VanBuren, R., and McLetchie, D.N. (2021). Expression dynamics of dehydration tolerance in the tropical plant *Marchantia inflexa*. Plant J. **105:** 209–222.

Martin, M.V., Fiol, D.F., Sundaresan, V., Zabaleta, E.J., and Pagnussat, G.C. (2013). *oiwa*, a female gametophytic mutant impaired in a mitochondrial manganese-superoxide dismutase, reveals crucial roles for reactive oxygen species during embryo sac development and fertilization in *Arabidopsis*. Plant Cell **25:** 1573–1591.

Maxwell, K., and Johnson, G.N. (2000). Chlorophyll fluorescence—A practical guide. J. Exp. Bot. **51:** 659–668.

McLetchie, D.N., and Puterbaugh, M.N. (2000). Population sex ratios, sex-specific clonal traits and tradeoffs among these traits in the liverwort *Marchantia inflexa*. Oikos **90:** 227–237.

Merényi, Z., Virágh, M., Gluck-Thaler, E., Slot, J.C., Kiss, B., Varga, T., Geösel, A., Hegedüs, B., Bálint, B., and Nagy, L.G. (2022). Gene age shapes the transcriptional landscape of sexual morphogenesis in mushroom-forming fungi (Agaricomycetes). eLife **11:** e71348.

Park, J.H., Lee, S.Y., Kim, W.Y., Jung, Y.J., Chae, H.B., Jung, H.S., Kang, C.H., Shin, M.R., Kim, S.Y., Su'udi, M., et al. (2011). Heat-induced chaperone activity of serine/threonine protein phosphatase 5 enhances thermotolerance in *Arabidopsis thaliana*. New Phytol. **191:** 692–705.

Parmesan, C., and Yohe, G. (2003). A globally coherent fingerprint of climate change impacts across natural systems. Nature **421:** 37–42.

Perez-Riverol, Y., Bai, J., Bandla, C., García-Seisdedos, D., Hewapathirana, S., Kamatchinathan, S., Kundu, D.J., Prakash, A., Frericks-Zipper, A., Eisenacher, M., et al. (2022). The PRIDE database resources in 2022: a hub for mass spectrometry-based proteomics evidences. Nucleic Acids Res. **50:** D543–D552.

Rizhsky, L., Liang, H., Shuman, J., Shulaev, V., Davletova, S., and Mittler, R. (2004). When defense pathways collide. the response of *Arabidopsis* to a combination of drought and heat stress. Plant Physiol. **134:** 1683–1696.

Rojek, J., Tucker, M.R., Pinto, S.C., Rychłowski, M., Lichocka, M., Soukupova, H., Nowakowska, J., Bohdanowicz, J., Surmacz, G., and Gutkowska, M. (2021). Rab-dependent vesicular traffic affects female gametophyte development in *Arabidopsis*. J. Exp. Bot. **72:** 320–340.

Schiffthaler, B., Van Zalen, E., Serrano, A.R., Street, N.R., and Delhomme, N. (2023). Seiðr: Efficient calculation of robust ensemble gene networks. Heliyon **9:** e16811.

Smith, M.A., and Maravolo, N.C. (2004). The influence of spermine on the in situ expression of a protein kinase associated with senescence in *Marchantia polymorpha* thalli. Int. J. Plant Sci. **165:** 745–751.

Tan, Q.W., Lim, P.K., Chen, Z., Pasha, A., Provart, N., Arend, M., Nikoloski, Z., and Mutwil, M. (2023). Cross-stress gene expression atlas of *Marchantia polymorpha* reveals the hierarchy and regulatory principles of abiotic stress responses. Nat. Commun. **14:** 986.

Thuiller, W., Lavorel, S., Araújo, M.B., Sykes, M.T., and Prentice, I.C. (2005). Climate change threats to plant diversity in Europe. Proc. Natl. Acad. Sci. U. S. A **102:** 8245–8250.

Tougane, K., Komatsu, K., Bhyan, S.B., Sakata, Y., Ishizaki, K., Yamato, K.T., Kohchi, T., and Takezawa, D. (2010). Evolutionarily conserved regulatory mechanisms of abscisic acid signaling in land plants: Characterization of ABSCISIC ACID INSENSITIVE1-like Type 2C protein phosphatase in the liverwort *Marchantia polymorpha*. Plant Physiol. **152:** 1529–1543.

Valledor, L., Escandón, M., Meijón, M., Nukarinen, E., Cañal, M.J., and Weckwerth, W. (2014a). A universal protocol for the combined isolation of metabolites, DNA, long RNAs, small RNAs, and proteins from plants and microorganisms. Plant J. **79:** 173–180.

Valledor, L., Romero-Rodríguez, M.C., and Jorrin-Novo, J.V. (2014b). Standardization of data processing and statistical analysis in comparative plant proteomics experiment. In *Methods in Molecular Biology. Plant Proteomics*, J.V. Jorrin-Novo, S. Komatsu, W. Weckwerth, S. Wienkoop, eds, (Totowa, NJ: Humana Press), pp. 51–60.

Valledor, L., and Weckwerth, W. (2014). An improved detergent-compatible gel-fractionation LC-LTQ-Orbitrap-MS workflow for plant and microbial proteomics. In *Methods in Molecular Biology. Plant Proteomics*, J.V. Jorrin-Novo, S. Komatsu, W. Weckwerth, S. Wienkoop, eds, (Totowa, NJ: Humana Press), pp. 347–358.

Van Der Does, D., Boutrot, F., Engelsdorf, T., Rhodes, J., McKenna, J.F., Vernhettes, S., Koevoets, I., Tintor, N., Veerabagu, M., Miedes, E., et al. (2017). The Arabidopsis leucine-rich repeat receptor kinase MIK2/LRR-KISS connects cell wall integrity sensing, root growth and response to abiotic and biotic stresses. PLoS Genet. **13:** e1006832.

Wimalasekera, R., Schaarschmidt, F., Angelini, R., Cona, A., Tavladoraki, P., and Scherer, G.F.E. (2015). *POLYAMINE OXIDASE2* of *Arabidopsis* contributes to ABA mediated plant developmental processes. Plant Physiol. Biochem. **96:** 231–240.

Wu, T.-Y., Hoh, K.L., Boonyaves, K., Krishnamoorthi, S., and Urano, D. (2022a). Diversification of heat shock transcription factors expanded thermal stress responses during early plant evolution. Plant Cell **34:** 3557–3576.

Wu, T.-Y., Krishnamoorthi, S., Boonyaves, K., Al-Darabsah, I., Leong, R., Jones, A.M., Ishizaki, K., Liao, K.-L., and Urano, D. (2022b). G protein controls stress readiness by modulating transcriptional and metabolic homeostasis in *Arabidopsis thaliana* and *Marchantia polymorpha*. Mol. Plant **15:** 1889–1907.

SUPPORTING INFORMATION

Additional Supporting Information may be found online in the supporting information tab for this article: http://onlinelibrary.wiley.com/doi/10.1111/jipb.13753/suppinfo

Figure S1. Post-stress phenotypic monitoring in Tak-1 and Tak-2

Figure S2. MOFA related information

Figure S3. Phenotypical monitoring of stress assay in additional natural accessions
Table S1. Photosynthetic measurements and biochemical marker quantification
Table S2. Protein identification, quantification, annotation, and descriptive analyses
Table S3. Latent factor analyses from ungrouped and multi-grouped frameworks
Table S4. Meta-networks and related information
Table S5. Evolutionary proteomics by protein gene age evaluation
Table S6. Targeted transcriptomics